Electronic structure of TiO_x $(0.8 < x < 1.3)$ with disordered and ordered vacancies

S. R. Barman and D. D. Sarma*
Solid State and Structural Chemistry Unit, Indian Institute of Science, Bangalore 560 012, India
(Received 20 July 1993; revised manuscript received 29 December 1993)

We report x-ray photoemission, UV photoemission, and bremsstrahlung isochromat spectra of TiO with ordered vacancies in both Ti and O sublattices and of the series TiO_x $(0.8 < x < 1.3)$ containing disordered Ti and O vacancies. The details of the electronic structure are discussed in comparsion to band-structure calculations for the ordered structures performed in this work as well as to density of states obtained for the disordered systems within different approximate methods reported earlier in the literature. Our results in the valence-band regions indicate the need for a better theoretical approach to describe the effect of disordered vacancies on the electronic structure than has been attempted to date. Ti $2p$ core-level spectra indicate the existence of vacancy-induced local environments with the formal charge on the Ti atom ranging from 2+ to 4+.

I. INTRODUCTION

The properties of TiO, a refractory transition-metal oxide, are of interest both from technological and theoretical viewpoints. This material is hard and brittle like a typical covalent refractory material,[1,2] while it is also metallic[3-6] with a resistivity of a few hundred $\mu\Omega$ cm at the lowest temperatures. The conduction band in TiO is primarily due to the direct overlap of neighboring Ti $3d$ orbitals of t_{2g} symmetry along the face diagonals of the rocksalt structure. On the other hand, the refractory properties of the oxide are due to the covalent bonding arising from the interaction of the O $2p$ and the Ti $3d$ orbitals of e_g symmetry along the edge of the cube. Thus, both the cation-cation bond and the cation-anion bond play important roles in determining the properties of this compound. The intra-atomic Coulomb interaction strength U_{dd} in the Ti $3d$ manifold is expected to be small compared to the Ti $3d$ conduction-band width,[7] suggesting that the independent-particle band description may provide a reasonable basis for discussing the electronic structure of this compound. The band structure for rocksalt stoichiometric TiO without vacancies has been reported by several authors.[8-14]

Another interesting aspect of TiO is that it forms over an extraordinarily wide homogeneity range. Thus, TiO_x can be formed with $0.8 < x < 1.3$ retaining the rocksalt structure.[3] The system is stabilized by an equilibrium concentration of vacancies which are randomly distributed in both the Ti and O sublattices. The anionic vacancy concentration decreases while the cationic vacancy concentration increases with increasing x. The total vacancy concentration, however, decreases with increasing x. It is interesting to note that even the compound with the nominal composition $TiO_{1.0}$ contains 15% random vacancies at both the Ti and O sites. It should be noted that the rocksalt phase of TiO_x exists only above 1250 °C, but can be stabilized at room temperature by quenching from temperatures above 1250 °C. Between 1250 °C and 940 °C a β-TiO phase, showing cubic superstructures, is stable.[15] However, annealing below 940 °C causes an ordering of the random vacancies along with slight distortion of the cubic symmetry in the rocksalt structure, leading to a monoclinic unit cell.[15-17] This structure has 16.7% cation and anion vacancies appearing in every third (110) plane of the rocksalt structure.[16] Thus, these compounds are very suitable for a systematic investigation of the effect of disordered vis-à-vis ordered vacancies on the electronic structure. The effect of ordered and disordered vacancies on the transport properties of TiO_x, controlled by a small energy scale around E_F, has been extensively investigated.[3-6] The primary source of electron scattering at low temperatures has been identified to be the Ti and O vacancies in the lattice.[6] The temperature coefficient of resistivity in these compounds[3-6] can be either positive or negative over a wide range of temperature depending on the vacancy concentration.

There have been several theoretical efforts to describe the influence of the vacancies on the electronic structure of TiO_x.[18-24] Schoen and Denker[18] calculated the band structure for TiO_x with different concentration of disordered vacancies $(0.8 < x < 1.22)$ in both the sublattices, using the augmented plane wave–virtual crystal approximation (APW-VCA). These authors find that (i) the energy gap (referred to as the p-d gap) between the primarily O $2p$ density of states (DOS) and the Ti $3d$ DOS increases with increasing x; (ii) there is no systematic dependence of the integrated intensity ratio (referred to as the d/p ratio) between the primarily Ti $3d$ DOS and the O $2p$ DOS with x; (iii) the vacancy bands do not appear even for vacancy concentrations as high as 20%; (iv) there are modifications in the shape and energy position in the unoccupied Ti $3d$ DOS with increasing x; and (v) the rigid-band model is inapplicable to describe the electronic structure of these systems. In a qualitative discussion of the influence of vacancies on the electronic structure, Goodenough argued[19] that (i) two holes are trapped in the cation vacancy, while two electrons are trapped in the anion vacancy, and (ii) the Ti $3d$ conduction band broadens with increasing vacancy concentration leading to an energy stabilization. However, based on the Korringa-Kohn-Rostoker (KKR) average t-matrix ap-

proximation (KKR-ATA) calculations[20] for vacancy-disordered $TiO_{1.0}$ with 15% vacancies (referred to in Ref. 20 as $Ti_{0.85}O_{0.85}$), Huisman, Carlsson, and Gellat concluded that (i) the vacancy-induced defect states appear below the Fermi energy filling the p-d gap, in contradiction to Ref. 18; (ii) the primarily Ti $3d$ derived conduction band becomes narrower in presence of vacancies, in contradiction to the suggestion in Ref. 19; and (iii) the mean energy of the O $2p$ band rises and that of the primarily Ti $3d$ derived conduction band becomes lower. The competition between the stabilizing effect of the defect states below E_F and the destabilizing effect due to the narrowing of the Ti $3d$ band and shift in the mean energies of the Ti $3d$ and O $2p$ DOS results in a finite concentration of vacancies in TiO. Gubanov *et al.*[21] have studied the effect of isolated vacancies in TiO_x by the nonempirical Hartree-Fock-Slater (HFS) method in the cluster approximation. These authors suggest that the vacancies cause (i) narrowing of bands, (ii) appearance of vacancy states in the unoccupied parts of the DOS, and (iii) the valency of the metal atom to vary continuously with x, suggesting a systematic change in the d/p ratio. Ivanovsky *et al.*,[22] based on the linearized-muffin-tin-orbital–Green's-function (LMTO-GF) approach, studied the electronic states induced by isolated vacancies. Their results suggest (i) formation of vacancy states below E_F; and (ii) decrease in the d/p ratio with increasing x. Burdett and Hughbanks[23] have explained the structure of vacancy-ordered TiO_x based on the results from semiempirical extended Hückel band-structure calculations. The DOS in Ref. 23 for vacancy-ordered TiO shows the absence of the p-d gap. Hobiger *et al.*[24] have performed self-consistent linear augmented-plane-wave (LAPW) band-structure calculations for hypothetical $Ti_{0.75}O_{0.75}$ crystallizing in the NbO structure. These authors find the absence of the p-d gap in this compound. Thus, from the above discussion it appears that there is no general consensus concerning the effect of vacancies on the electronic structure of TiO_x, though a large number of calculations have been performed for this system. It is to be noted that much of the above predictions of the calculations can be experimentally verified by investigating the electronic structure of TiO_x using techniques of high-energy electron spectroscopies. Surprisingly, there have been only a few such experiments on a limited range of x values in TiO_x, and the above-stated conflicting descriptions of the electronic structure of TiO_x could not be resolved on the basis of these experiments.

An early x-ray photoemission (XP) study on $TiO_{1.1}$ by Wertheim and Buchanan[25] clearly showed the Ti $3d$ conduction band well separated from the O $2p$–Ti $3d$ hybridized band, suggesting the existence of a p-d gap. These authors however did not investigate any other composition, and thus did not address the question of the effect of vacancies on the electronic structure. On the other hand, the x-ray emission (XE) spectra do not indicate[26] the existence of a p-d gap in the TiO_x series. The XE spectra suggest that the primarily O $2p$ band-related feature shifts towards lower binding energy and the d/p ratio decreases systematically with increasing x. Contrasting this result, the ultraviolet photoemission (UP) spectra[27] do not show any significant difference between the two different compositions $TiO_{0.93}$ and $TiO_{1.15}$. Thus we felt that a systematic investigation of the electronic structure of TiO_x for various x would be worthwhile, particularly if a careful comparison could be made to the calculated density of states. We present in this paper a detailed spectroscopic study of the electronic structure of TiO_x ($x=0.81$, 0.91, 1.03, 1.18, 1.30) with disordered vacancies, as well as one sample of TiO ($x=1.0$) with ordered vacancies. We study the occupied and unoccupied parts of the density of states of TiO using XP, UP, and bremsstrahlung isochromat (BI) spectroscopic techniques. We also investigate the Ti $2p$ and O $1s$ core-level XP spectra. In order to compare and interpret the experimental results, we have calculated the DOS and various site- and angular-momentum projected partial DOS (PDOS) within the linearized muffin-tin orbital–atomic-sphere approximation (LMTO-ASA) for the vacancy ordered TiO ($V_{Ti}=V_O=16.7\%$). We have also calculated the DOS and the various PDOS for the rocksalt stoichiometric TiO without vacancies. Besides providing a description for the electronic structure of TiO, in this work we attempt to address various questions regarding the effects of vacancies on the electronic structure of TiO based on experiment and calculations, with specific reference to the p-d gap and d/p ratio.

II. EXPERIMENT

The TiO_x ($0.8<x<1.3$) samples with disordered vacancies were prepared by melt-quenching a mixture of Ti and TiO_2 in the required proportions in an arc furnace under inert argon atmosphere. The monoclinic vacancy-ordered phase of TiO was obtained by annealing a disordered sample of $TiO_{1.0}$ at 900 °C for 48 h in vacuum.[17] Powder x-ray diffraction and resistivity measurements were carried out to characterize the samples. The variation of the lattice constant with x and the resistivity measurements agree well with the published data.[17] The oxygen stoichiometry (x) was determined by measuring the increase in the weight on oxidizing the samples to TiO_2 at 1000 °C in flowing oxygen. The estimated compositions were found to be $TiO_{0.81}$, $TiO_{0.91}$, $TiO_{1.03}$, $TiO_{1.18}$, and $TiO_{1.30}$, corresponding to the starting compositions with $x=0.8$, 0.9, 1.0, 1.15, and 1.28, respectively.

The electron spectroscopic experiments were carried out in a combined XPS-UPS-BIS spectrometer from VSW Scientific Limited, U.K. A clean and reproducible sample surface was obtained by scraping the sample with an alumina file in a vacuum of 5×10^{-10} mbar until the various core levels did not show any further change. The cleanliness of the surface was further monitored by recording the C $1s$ and O $1s$ spectral regions. While the O $1s$ spectrum was found to have a single peak, the signal due to C $1s$ was negligible for the scraped surfaces. All the experiments were carried out at the liquid-nitrogen temperature to minimize surface degradation with time. However, the spectra recorded at room temperature were identical to those recorded at the low temperature for

freshly scraped surfaces. The instrumental resolution for the XPS measurements with nonmonochromatic Mg $K\alpha$ radiation is 0.8 eV, while the resolution for He I UPS measurements is 140 meV. The resolution for BIS is 0.8 eV.

The total DOS and the angular-momentum-projected PDOS calculation for rocksalt TiO without vacancies and for vacancy-ordered TiO with $V_{Ti} = V_O = 16.7\%$ were performed within LMTO-ASA. In the LMTO method, an energy-independent, fixed-basis set is constructed from the partial waves and their first energy derivatives obtained within the muffin-tin approximation to the potential. The effective potential in the solid is modeled by constructing spheres around each atomic site. The potential within the spheres is assumed to be spherically symmetric, while the potential in the interstitial region is assumed to take a constant value. Within the ASA approximation, the atomic spheres are taken to be slightly overlapping so that the volume of the spheres in a unit cell add up to the total volume of the unit cell. Thus in this case, the interstitial region is eliminated. If this space-filling requirement in ASA requires unphysically large overlap of spheres, additional empty spheres are introduced in the interstitial regions. In the case of vacancy-ordered TiO, the unit cell is monoclinic (space group $A2/m$) with $a = 5.855$ Å, $b = 9.34$ Å, $c = 4.142$ Å, and $\gamma = 107° 32'$ (Ref. 16). The unit cell consists of ten atoms of titanium and ten atoms of oxygen. In the LMTO-ASA calculation empty spheres were included for two vacancies of Ti and two vacancies of O in each unit cell. The self-consistent calculations were performed with 145 k points for the vacancy-ordered structure in the irreducible part of the Brillouin zone. The energies E_ν^l for each partial wave were chosen to be the center of gravity of the occupied parts of the corresponding partial DOS.

III. RESULTS AND DISCUSSION

We show the x-ray and He II photoelectron valence-band spectra from vacancy-ordered TiO in Fig. 1(a), with a higher resolution He I UP spectrum in the near-E_F region as an inset. The spectra exhibit two distinctly separated features, one within the first 3 eV of E_F, while the other one is centered around 7.3 ± 0.3 eV, in close similarity with the results for $TiO_{1.1}$ using XPS,[25] and for $TiO_{0.93}$ and $TiO_{1.15}$ using UPS.[27] In agreement with the earlier works,[25–27] we interpret the peak close to E_F as arising primarily from Ti 3d and the peak at 7.3 eV due to mainly O 2p-like states. This is also consistent with the observed increase in the relative intensity of the feature near E_F with the photon energy [Fig. 1(a)], as the cross section of the Ti 3d states is expected[28] to increase compared to the O 2p states with increasing photon energy. Both the spectra in Fig. 1(a) show a finite intensity at E_F with a clear Fermi cutoff observable in the high-resolution UP spectrum. In order to interpret the electronic structure and bonding in TiO, we have calculated the total and partial DOS for the vacancy-ordered TiO_x [Fig. 1(b)], since such a calculation does not exist in the literature. From Fig. 1(b) we find that the states near the

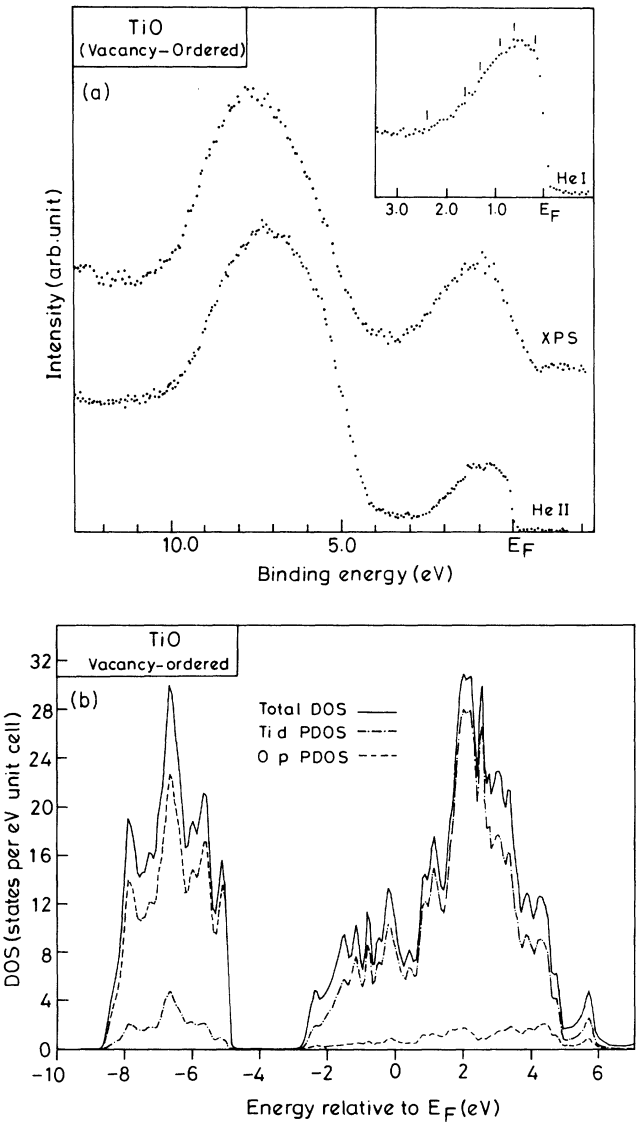

FIG. 1. (a) XP and He II UP spectra of vacancy-ordered TiO. He I UP spectrum in the near E_F region is shown in the inset; the energy positions of the various features in the calculated DOS in (b) are marked in the inset (see text). (b) The total DOS (solid line), Ti d (dot-dashed line), and O p (dashed line) partial DOS for vacancy-ordered TiO calculated within LMTO-ASA.

Fermi energy are primarily due to Ti 3d states. This indicates that the metallic property of TiO is derived primarily from Ti 3d–Ti 3d t_{2g} σ interaction. Similarly, the higher-binding-energy feature 6.8 ± 0.3 eV below E_F in Fig. 1(b) corresponds primarily to O 2p derived bands, though there is some Ti 3d admixture over the entire bandwidth. This admixture is evidenced by the presence of Ti d PDOS in the 5–8.5 eV range below E_F [Fig. 1(b)] mimicking the O p PDOS features at the same energy. This illustrates the importance of covalent interaction in the bonding of TiO which arises primarily from Ti 3d e_g–O 2p σ interactions. We find from Fig. 1(b) that the calculated DOS has various features at about -0.2, -0.6, -0.9, and -1.3 eV with respect to E_F. These

features are essentially due to structures in the Ti $3d$ partial DOS which accounts for more than 70% of the contribution to the DOS in this energy range. There are two other features in the calculated DOS at -1.6 and -2.4 eV. The PDOS corresponding to the states in the empty spheres considered at the oxygen vacancy sites [not shown in Fig. 1(b)] contribute significantly only to these two features along with the Ti d PDOS contribution. In this sense, these two features at -1.6 and -2.4 eV are oxygen-vacancy-induced states. Thus we find that the vacancy-induced states appear below E_F, in agreement with the KKR-ATA (Ref. 20) and LMTO-GF (Ref. 22) calculations and the suggestion[19] that oxygen vacancies will trap electrons. However, these vacancy-induced states, though appearing at the bottom of the conduction band, do not wipe out the p-d gap [Fig. 1(b)]. In the present calculation with the real structure, the energy position of the O $2p$ related DOS at 6.8 ± 0.3 eV compares well with that of the experimental value of 7.3 ± 0.3 eV. Also, the calculated Ti $3d$ occupied DOS extends to about 2.8 eV below E_F [Fig. 1(b)], in good agreement with the experimentally estimated value of 2.8 ± 0.3 eV [Fig. 1(a)], suggesting the absence of any strong correlation effects. We attempted to estimate the strength of U_{dd} from an analysis of the Ti L_{23}-$M_{45}M_{45}$ Auger spectrum; however, the Auger spectrum compares well with the self-convoluted Ti $3d$ XP spectrum indicating the absence of any intense spectral features due to two correlated d holes. This confirms that U_{dd} is indeed small in TiO. In order to compare the calculated Ti $3d$ DOS and the experimental He I UP spectra, we have marked in the inset of Fig. 1(a) the energy positions of the various features from the calculated DOS in Fig. 1(b). It appears that the features in the DOS at -0.2, -0.6, and -0.9 eV have their corresponding counterparts in the experimental spectra, though the features are weak and barely above the noise level. Further experiments with higher resolution and better intensity, for example, with the use of synchrotron radiation, are desirable to establish these points. The features further away from E_F at -1.3, -1.6, and -2.4 eV are not seen in the experimental spectra; the reason for this is the increased lifetime broadening at higher binding energies coupled with the problems of resolution and intensity as mentioned above.

The electronic structure of TiO has often been described in the past in terms of the stoichiometric rocksalt structure without vacancies.[8-14] The calculated total DOS and the O $2p$ and Ti $3d$ partial DOS for the rocksalt TiO without vacancies are shown in Fig. 2; the results here are in agreement with previously published data.[10] Comparing these results with those for vacancy-ordered TiO [Fig. 1(b)], we find that there are some important disagreements between the two. For example, the calculated DOS near E_F in Fig. 2 is such that the experimental spectrum would be expected to give rise to a single peak at E_F broadened by the resolution function and lifetime effects, with no other spectral features within the first 6 eV, in contrast to the DOS for the vacancy-ordered structure [Fig. 1(b)] as well as the experimental spectra [Fig. 1(a)], which show the Ti $3d$ related peak away from the E_F. Another significant discrepancy between the calculation for the rocksalt TiO and the experiment is that the calculated result in Fig. 2 exhibits an occupied Ti $3d$ bandwidth of nearly 4.2 eV, while the valence-band spectra in Fig. 1(a) and the calculated result in Fig. 1(b) suggest a much smaller (2.8 eV) value. Moreover, for the vacancy-ordered structure, the total Ti $3d$ bandwidth is 8.8 eV compared to 11 eV in the rocksalt structure with no vacancies. Thus, it appears that the decreased coordination in the vacancy-ordered structure dominates over the effects caused by a decrease in the bond lengths, leading to a narrowing of the bandwidth in contrast to the suggestion in Ref. 19. The peak position of the calculated O $2p$ partial DOS in Fig. 1(b) is 6.8 eV, while that for the rocksalt TiO (Fig. 2) is near 8.5 eV, indicating a decrease in energy separation between the O $2p$ and Ti $3d$ DOS in the presence of vacancies. Thus, it appears that the details of the electronic structure of TiO are strongly influenced by the presence of vacancies. Compared to the stoichiometric rocksalt TiO without vacancies, the presence of vacancies leads to a narrowing of the d-band width, decrease in energy separation between the O $2p$ and Ti $3d$ DOS, and appearance of sharp structures over the entire range of the DOS. Such sharp structures in the DOS close to E_F suggest the interesting possibility of affecting the physical properties of the system by shifting the E_F slightly, for example, by changing x in TiO_x. This may be partly responsible for the interesting changes ob-

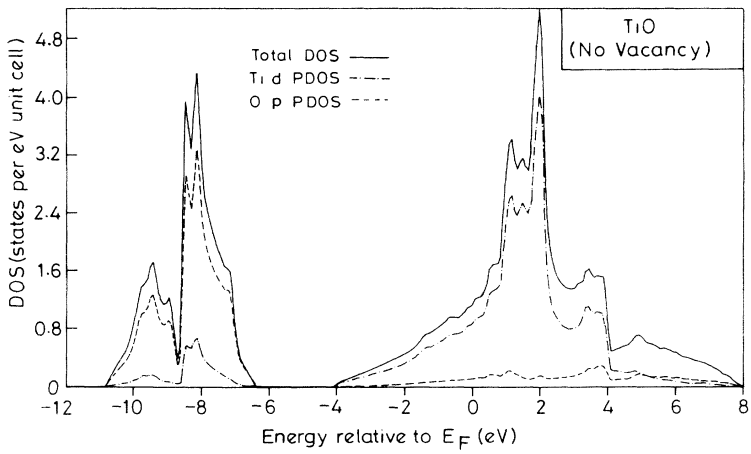

FIG. 2. The total DOS (solid line), Ti d (dot-dashed line), and O p (dashed line) partial DOS for stoichiometric rocksalt TiO with no vacancies calculated within LMTO-ASA.

served in the transport properties of these systems.[3–6]

We show the UP and XP spectra of vacancy-disordered TiO_x with $x = 0.81$, 0.91, 1.03, 1.18, and 1.30 in Figs. 3(a) and 3(b). The comparison of the spectral features of vacancy-ordered TiO [Fig. 1(a)] with vacancy-disordered $TiO_{1.03}$ [Figs. 3(a) and 3(b)] suggests that the long-range ordering of the vacancies does not alter the spectral features very much. The only discernible difference in the shape near E_F between the spectra of the ordered and disordered vacancy systems appears to be a slight broadening in the disordered phase [inset, Figs. 1(a) and 3(a)]. This is not surprising in view of the results of diffuse x-ray[29] and electron[30] diffraction experiments which reveal that the local atomic arrangements in the disordered phase partially resemble the vacancy-ordered phase. The experimental p-d gap for the vacancy-disordered TiO_x is somewhat more than 1 eV. The same gap, within experimental uncertainties, is also observed in the experimental spectrum of the vacancy-ordered TiO [Fig. 1(a)]. The present results are in contrast to the KKR-ATA (Ref. 20) calculations suggesting the absence of any gap. The XE spectra[26] for TiO_x also do not indicate the existence of the p-d gap in contrast to the present results. Our results, however, suggest that the p-d gap exists for all compositions of vacancy-disordered TiO_x and is relatively insensitive to the oxygen content (Fig. 3). The APW-VCA (Ref. 18) calculations which show the existence of the gap, however, indicate an increase in the gap with increasing x. From the spectra in Fig. 3, it is clear that the primarily O $2p$ derived spectral features are nearly identical in the entire TiO_x series with a similar width and peak position at 7.3 eV. In this regard the experimental value is in good agreement with the results of KKR-ATA (Ref. 20) showing the O $2p$ centroid at about 7 eV. The invariance in the O $2p$ peak position is in contrast to the APW-VCA (Ref. 18) results, which showed a systematic increase in the binding energy of the O $2p$ related feature (5.2 eV for $TiO_{0.8}$ to 6.9 eV for $TiO_{1.22}$). Interestingly, the XE (Ref. 26) results suggest an opposite trend of the O $2p$ related feature moving towards E_F with increasing x. One of the possible reasons for the discrepancies between the XE spectra and the present results is that the Ti $K\beta_5$ XE spectra are primarily sensitive to the Ti p partial DOS, whereas the photoemission spectra in Fig. 4 are primarily sensitive to the Ti $3d$ and O $2p$ states, which are the main constituents of the DOS below E_F. It is evident from Fig. 3(b) that the intensity of the Ti $3d$-like states shows marked decrease with increasing x. We have calculated the ratio of the integrated intensities from the Ti $3d$ and O $2p$ related spectral regions. We find the d/p ratio [inset, Fig. 3(b)] decreases monotonically with increasing x. A similar behavior is also observed for the He II UP spectra [Fig. 3(a)]. This decrease in the d/p ratio is related to the decrease of Ti concentration relative to O across the series; this effect is also responsible for the weakening of the Ti $3d$–Ti $3d$ metallic bond. This leads to a decrease in the density of states at E_F and is responsible for the increase in the resistivity of TiO_x with increasing x. We also find that the d/p ratio appears to be higher in the vacancy-

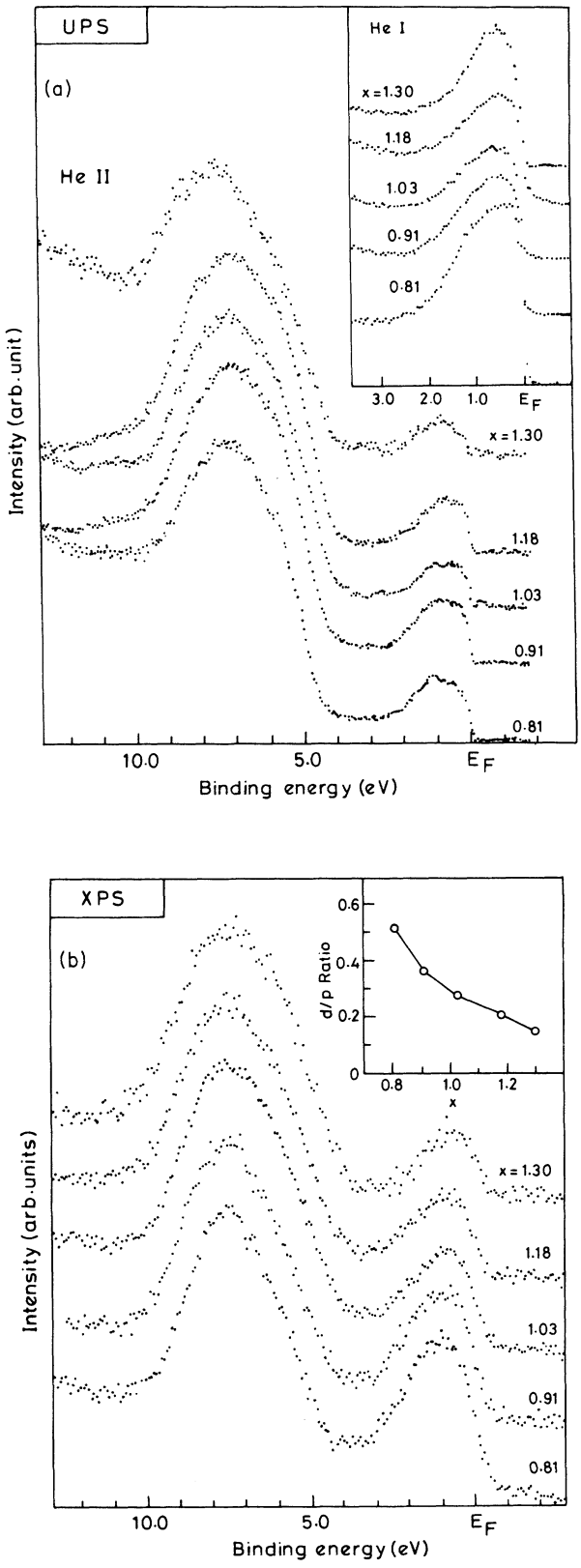

FIG. 3. (a) He II UP spectra for vacancy-disordered TiO_x ($0.8 < x < 1.3$). The inset shows the He I UP spectra for the same series in the near-E_F region. (b) XP spectra for vacancy-disordered TiO_x; the inset shows the change in the d/p ratio as a function of x (see text).

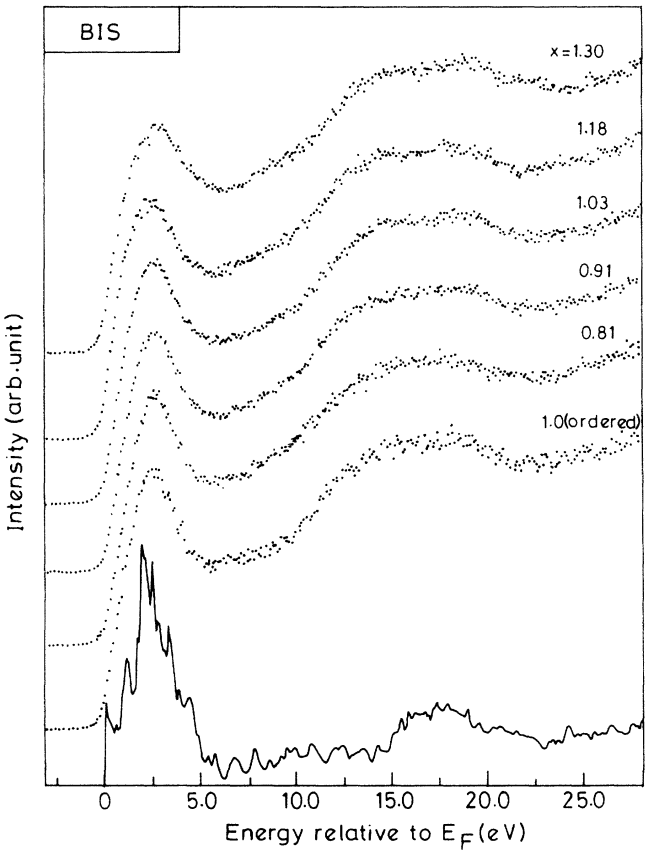

FIG. 4. BI spectra of vacancy-disordered TiO_x ($0.8 < x < 1.3$) and vacancy-ordered TiO, compared with the calculated DOS above E_F for the vacancy-ordered TiO.

ordered TiO compared to the vacancy-disordered $TiO_{1.03}$, though both have similar vacancy concentrations. This suggests a more effective metallic bonding in the vacancy-ordered TiO, the resistivity[3] of the vacancy-ordered TiO being lower by a factor of 4 compared to the vacancy-disordered TiO_x at 77 K. The decrease of the d/p ratio with increasing x is in agreement with the results of HFS cluster[21] and LMTO-GF (Ref. 22) calculations. The XE data[26] also show a similar trend. On the other hand, this result is in contrast to the APW-VCA (Ref. 18) calculations, which show no such correlation.

We show the BI spectra of vacancy-disordered TiO_x along with vacancy-ordered TiO in Fig. 4. We have calculated the unoccupied part of the DOS and PDOS for vacancy-ordered TiO (Fig. 4) by shifting all the E_v^l's (except for Ti d and O p states) to about 10 eV above E_F. The calculated DOS is found to be in gross agreement with the corresponding experimental spectrum; the differences in the relative intensities of the various features are due to matrix-element effects. From the calculated PDOS (not shown in the figure), we find that the experimentally observed peak at 2.4 ± 0.3 eV in BIS arises primarily from Ti $3d$ states. Its shape, with a relatively low intensity at E_F, is consistent with the calculated DOS. The calculation indicates that the Ti $3d$ band extends to about 6 eV above E_F; this is in agreement with the dip in the experimental spectrum at the same energy. The rise of the spectrum beyond this dip (Fig. 4) is due to the presence of Ti s,p and O s,d states. Specifically, the broad peak in the experimental spectrum between 15 and 20 eV above E_F arises primarily from O d and Ti p states. From Fig. 4 we find that the BI spectral features are very similar for the ordered and vacancy-disordered TiO, as in the case of the XP and UP data. This is in contrast to the suggestion[19] that the DOS just above E_F distorts considerably on the formation of disordered vacancies compared to the DOS of vacancy-ordered TiO. It is seen from Fig. 4 that the spectra of vacancy-disordered TiO_x for different x are remarkably similar. This observation is in contradiction to the results of APW-VCA (Ref. 18) calculations, which suggest that the Ti $3d$ peak position in the unoccupied part of the DOS appears between 1.9 and 3.2 eV, depending on x. Moreover, the calculation[18] also suggests considerable variation in the spectral shape as a function of x, which is not in agreement with the present data. It is to be noted that the similar spectral features for the Ti $3d$ states, and in particular the absence of any shift in the peak position, suggest the inapplicability of any rigid bandlike model for TiO_x. Though the various spectra in Fig. 4 are very similar, there are small changes that can be observed. For example, from a comparison of the two extreme stoichiometries $x=0.81$ and 1.30, we find that the dip in the spectral intensity at 6 eV above E_F is less pronounced in the sample with the higher oxygen content. This change is accompanied with a progressive increase in a spectral feature at about 13.5 eV with increasing x. This leads to the change from a broad single-peak feature for $TiO_{0.81}$ at about 16 eV to a two-peak feature in samples with higher x (Fig. 4). We point out here that the BI spectrum for vacancy-disordered $TiO_{1.1}$ reported earlier[31] appears different from the present spectrum. In the earlier spectrum, the intensity of the Ti $3d$ related feature and the dip at 6 eV are less pronounced and the shape of the high-lying states is different. These differences possibly arise from contamination of the sample surface, as the sample was not cleaned *in situ* in the previous work.

While the valence-band photoemission and BI spectra exhibit minor changes with x in TiO_x, the Ti $2p$ core-level spectra exhibit pronounced modifications across the series (Fig. 5). The $2p_{3/2}$ peak for the $x=0.81$ sample appears at 454.8 ± 0.2 eV binding energy. Two distinct effects can be observed in the spectra with increasing x; there is a systematic shift of the peak position to higher binding energy, and a broad feature develops at about 458 eV binding energy which gradually fills up the dip between the $2p_{3/2}$ and $2p_{1/2}$ peaks. Another broad and weaker feature also develops at about 464 eV binding energy. The shift of the main peak to higher binding energy with increasing x is attributed to a decrease in screening of the core-hole state, as suggested by the decrease of the Ti $3d$ band intensity near E_F in this series (Fig. 3). We find the O $1s$ spectrum in every case to be a single peak of 2 eV full width at half maximum with no extra features. This ensures that the spectral features at 458 eV and 464 eV in TiO_x are not due to surface degradation or contam-

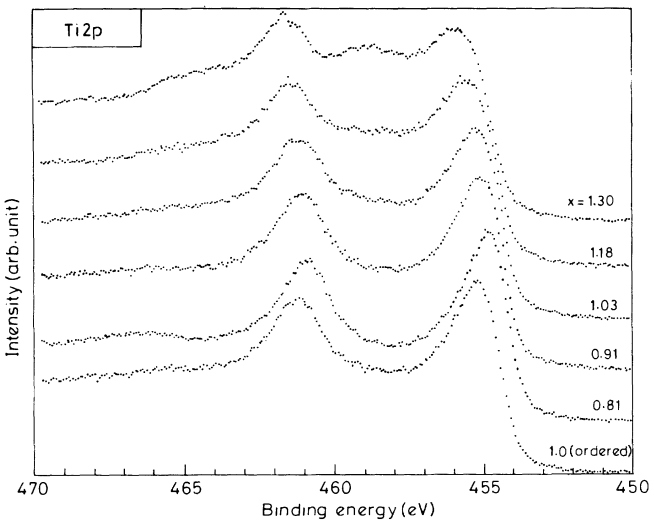

FIG. 5. Ti $2p$ core-level spectra of vacancy-disordered TiO_x ($0.8 < x < 1.3$) and vacancy-ordered TiO.

ination. However, the O $1s$ spectra exhibit a small overall shift of about 0.3 eV towards lower binding energy with increasing x. The spectral features emerging at 458 eV and 464 eV binding energies with increasing x appear to be broad compared to that in any stoichiometric oxide of titanium. Furthermore, the peak positions of these extra features are at a lower binding energy (by about 1 eV) compared to that in TiO_2. Thus, the spectral features suggest that local environments similar to the entire range of formal oxidation states from Ti^{2+} to Ti^{4+} (including the intermediate states) may be present in TiO_x. The local environments corresponding to the higher oxidation states increase with x, as evidenced by the increase of the higher binding energy features. The above suggestion is in agreement with the results of diffuse x-ray scattering studies,[29] indicating that a Ti ion in TiO_x tends to surround itself with both Ti and O vacancies. However, increasing x leads to a decrease in V_O and an increase in V_{Ti}. This then creates more numbers of Ti sites dominated by the presence of many Ti vacancies in the neighboring sites, leading to a local electronic structure determined primarily by Ti $3d$–O $2p$ covalent bonding at the expense of Ti $3d$–Ti $3d$ metallic bonding. This is consistent with the decrease in the d/p ratio with increasing x, as observed in the XP and UP spectra of TiO_x (Fig. 3). The broad features around 458 eV and 464 eV are also present in vacancy-ordered TiO, though less pronounced than in the case of vacancy-disordered $TiO_{1.03}$ (Fig. 5). This may be due to the fact that though the vacancy ordering in TiO does not allow clustering of Ti vacancies around a Ti ion, there are two different kinds of Ti ions in this compound with two and three Ti vacancies in the nearest-neighbor shell.

We conclude by summarizing our findings vis-à-vis the existing theoretical results on the TiO system. The gap between the O $2p$ and Ti $3d$ DOS (p-d gap) persists even in the presence of vacancy-induced states. This is in disagreement with the results of KKR-ATA,[20] semiempirical Hückel,[23] and LAPW (Ref. 24) calculations. Discrepancy with the LAPW calculation indicates the importance of including the realistic structural details in describing the electronic structure of vacancy-ordered TiO. The experimental data further indicate that the p-d gap remains invariant in TiO_x with changing x, in contradiction to the APW-VCA (Ref. 18) calculations. The spectra exhibit a systematic decrease in the d/p ratio in TiO_x with increasing x. The APW-VCA (Ref. 18) calculations, on the other hand, show no such correlation for the calculated d/p ratio. The vacancy states in the DOS calculation for vacancy-ordered TiO appear below E_F. However, this finding is in disagreement with the APW-VCA (Ref. 18) calculations where vacancy states do not appear, and the HFS cluster[21] calculation where the vacancy states are located above E_F. The experimental spectra for vacancy-ordered TiO and vacancy-disordered TiO_x suggest that the ordering of the vacancies does not alter the spectral features very much, in contradiction to the suggestions in Ref. 19. The BI spectra for TiO_x do not show major modifications with changing x in contrast to the results of the APW-VCA (Ref. 18) calculations. This observation also suggests the inapplicability of the rigid-band model in these compounds. We show that the presence of ordered vacancies in TiO leads to a narrowing of the Ti d band width. This is in disagreement with the suggestion[19] of a band broadening in the presence of vacancies. The Ti $2p$ core-level spectra show major modifications with changing x, indicating the existence of vacancy-induced local environments with the formal oxidation state of Ti ranging from 2+ to 4+. The changes in the Ti $2p$ core-level spectra are consistent with the systematic change in the d/p ratio observed in the valence-band spectra. Thus, in the present work we have studied the systematics in the electronic structure of the series TiO_x with $0.8 < x < 1.3$ containing disordered Ti and O vacancies, and compared these with the electronic structure of the vacancy-ordered TiO. Comparison of the present experiments with the results of earlier attempts to describe the effect of disordered vacancies on the electronic structure of these compounds indicates the need for a better theoretical approach than has been attempted to date.

ACKNOWLEDGMENTS

We thank Professor C. N. R. Rao for his continued support. Support for this work from the Homi Bhabha Fellowship Council and the Department of Science and Technology, Government of India, is gratefully acknowledged. We thank Dr. M. Methfessel, Dr. A. T. Paxton, and Dr. M. van Schiljgaarde for making the LMTO-ASA band structure program available to us. We thank Dr. S. Krishnamurthy and Dr. N. Shanthi for the initial help in setting up the LMTO-ASA program. S.R.B. is thankful for support from the Council of Scientific and Industrial Research, Government of India.

*Electronic address: sarma@sscu.iisc.ernet.in

[1]H. J. Goldshmidt, *Interstitial Alloys* (Butterworths, London, 1967).
[2]L. Toth, *Transition Metal Carbides and Nitrides* (Academic, New York, 1971).
[3]M. D. Banus, T. B. Reed, and A. J. Strauss, Phys. Rev. B **5**, 2775 (1972).
[4]S. P. Denker, J. Appl. Phys. **37**, 142 (1964).
[5]J. K. Hulm, C. K. Jones, R. A. Hein, and J. W. Gibson, J. Low Temp. Phys. **7**, 291 (1972).
[6]D. S. MacLachlan, Phys. Rev. B **25**, 2285 (1982).
[7]T. Bandyopadhyay and D. D. Sarma, Phys. Rev. B **39**, 3517 (1989).
[8]V. Ern and A. C. Switendick, Phys. Rev. **137**, A1297 (1965).
[9]L. F. Mattheiss, Phys. Rev. B **5**, 290 (1972).
[10]A. Neckel, P. Rastl, R. Eibler, P. Wienberger, and K. Schwarz, J. Phys. C **9**, 579 (1976).
[11]P. Blaha and K. Schwarz, Int. J. Quantum Chem. **23**, 1535 (1983).
[12]S. Kim and R. S. Williams, J. Phys. Chem. Solids **49**, 1307 (1988).
[13]J. L. Calais, Adv. Phys. **26**, 847 (1977).
[14]A. Neckel, Int. J. Quantum Chem. **23**, 1317 (1983).
[15]J. L. Murray and H. A. Wriedt, Bull. Alloy Phase Diagr. **8**, 148 (1987).
[16]D. Watanabe and J. R. Castles, Acta Crystallogr. **23**, 307 (1967).
[17]M. D. Banus and T. B. Reed, in *The Chemistry of Extended Defects in Non-Metallic Solids,* edited by M. O'Keeffe (North-Holland, Amsterdam, 1970), p. 488.
[18]J. M. Schoen and S. P. Denker, Phys. Rev. **184**, 864 (1969).
[19]J. B. Goodenough, Phys. Rev. B **5**, 2764 (1972).
[20]L. M. Huisman, A. E. Carlsson, and C. D. Gellat, Jr., Phys. Rev. B **22**, 991 (1980).
[21]V. A. Gubanov, A. L. Ivanovsky, G. P. Shveikin, and D. E. Ellis, J. Phys. Chem. Solids **45**, 719 (1983).
[22]A. L. Ivanovsky, V. I. Anisimov, D. L. Novikov, A. I. Lichtenstein, and V. A. Gubanov, J. Phys. Chem. Solids **49**, 465 (1988).
[23]J. K. Burdett and T. Hughbanks, J. Am. Chem. Soc. **106**, 3101 (1984).
[24]G. Hobiger, P. Herzig, R. Eibler, F. Schlappansky, and A. Neckel, J. Phys. Condens. Matter **2**, 4595 (1990).
[25]G. K. Wertheim and D. N. E. Buchanan, Phys. Rev. B **17**, 2780 (1978).
[26]K. Tsutsumi, O. Aita, and K. Ichikawa, Phys. Rev. B **15**, 4638 (1977).
[27]V. E. Henrich, H. J. Zeiger, and T. B. Reed, Phys. Rev. B **17**, 4121 (1978).
[28]J. J. Yeh and I. Lindau, At. Data Nucl. Data Tables **32**, 1 (1985).
[29]H. Terauchi and J. B. Cohen, Acta Crystallogr. Sec. A **35**, 646 (1979).
[30]R. de Ridder, D. van Dyck, G. van Tendeloo, and S. Amelinckx, Phys. Status Solidi A **40**, 669 (1977).
[31]F. Richle, Th. Wolf, and C. Politis, Z. Phys. B **47**, 201 (1982).